

# CNO cycle: "Soft E1" mode of the $^{17}\text{Ne}$ excitation in the $^{17}\text{Ne} + \gamma \rightarrow ^{15}\text{O} + 2p$ reaction.

Yu L Parfenova<sup>1,2</sup>, L V Grigorenko<sup>1,3,4</sup>, I A Egorova<sup>1</sup>, N B Shulgina<sup>3</sup>,  
M V Zhukov<sup>6</sup>

<sup>1</sup> JINR, Dubna, Russia

<sup>2</sup> INP MSU, Moscow, Russia

<sup>3</sup> RRC KI, Moscow, Russia

<sup>4</sup> GSI Helmholtzzentrum für Schwerionenforschung, Darmstadt, Germany

<sup>6</sup> Chalmers University of Technology, Göteborg, Sweden

E-mail: parfenova@jinr.ru

**Abstract.** The  $^{15}\text{O}(2p,\gamma)^{17}\text{Ne}$  reaction is studied using the time-reversed reaction of the  $^{17}\text{Ne}$  E1 Coulomb dissociation on lead target in the context of nuclear astrophysics. Looking for the relation between the data on the Coulomb excitation and the astrophysical 2p-capture rate, one faces problem to extract the Coulomb E1 strength function from the measured Coulex cross section. We use a number of phenomenological approaches to estimate influence of such processes as Coulomb-nuclear interference, populations of states with different  $J^\pi$ , etc. We calculate the  $^{17}\text{Ne} + 2p$  astrophysical capture rate and compare the results with different calculations.

## 1. Introduction

The last decade, studies of proton-rich nuclei in the vicinity of the drip-lines are a subject of intensive experimental and theoretical investigations. In particular, the study of a candidate to the two-proton Borromean halo nucleus  $^{17}\text{Ne}$  ( $^{15}\text{O} + p + p$  where all binary subsystems are unbound) in dissociation reactions, is of a special interest (see discussions in [1, 2, 3]). In particular, the study of the  $^{17}\text{Ne}$  Coulomb break-up can provide a information on  $^{15}\text{O}(2p,\gamma)^{17}\text{Ne}$  reaction rate, that is interesting from the astrophysical view point. According to the detailed balance theorem, the 2p-capture reaction can be accessed as the time-reversed one for E1 Coulomb dissociation of  $^{17}\text{Ne}$  in heavy target. Knowing the  $^{17}\text{Ne}$  excitation spectrum for E1 Coulomb excitation, one can get the E1 strength function, and then make a conclusion on the astrophysical  $^{15}\text{O} + 2p$  capture rate.

Recently, the  $^{17}\text{Ne}$  Coulomb break-up on lead target has been experimentally studied at GSI with LAND setup (experiment S318, 2006) [4]. Analyzing these data and aiming to find the relation between the experimental data on the Coulomb excitation and the astrophysical 2p-capture rate we face a set of problems.

First of all, the "soft E1" mode (SDM) [5] is not well studied for excitations of proton-rich nuclei. For example, theoretically predicted strength functions significantly differs depending on the calculation models (see, for example calculations in cluster model [6] and in collective RPA model [7]).



Another considerable uncertainty concerning the interpretation of SDM excitation is related to the yet unknown mixture of the  $[s^2]$  and  $[d^2]$  proton configurations in the  $^{17}\text{Ne}$  ground state wave function (WF).

Studying the time-reversed reaction of the  $^{17}\text{Ne}$  dissociation in the context of nuclear astrophysics, it is necessary to extract the information on the Coulomb-induced E1 dissociation from a wide set of different processes contributing to the  $^{15}\text{O}$  production, i.e. nuclear- induced dissociation, proton removal from the  $^{15}\text{O}$  core fragment in  $^{17}\text{Ne}$  [8] contributing to the total proton removal in  $^{17}\text{Ne}$  up to 30% [9], and etc.

When both Coulomb and nuclear mechanisms act, the question unavoidably arise on the Coulomb-nuclear interference which is also poorly studied and may influence the  $^{17}\text{Ne}$  excitation spectrum and angular distribution of the  $^{17}\text{Ne}$  fragments.

Also, contributions of different  $E\lambda$  and  $N\lambda$  transitions in vicinity of SDM peak are not yet understood.

Here, we focus on several of these problems, i.e. (i) the nuclear dipole (N1) excitation of  $^{17}\text{Ne}$  in lead and carbon targets, (ii) the Coulomb-nuclear interference for electric dipole (E1) and nuclear dipole (N1) excitations, and (iii) the astrophysical  $^{15}\text{O}+2p$  capture rate. For the calculations, a combined approach based on convenient models for description of the Coulomb and nuclear- induced reactions with clusterized systems, is used.

## 2. Model

This combined approach is based on the model of Bertulani and Baur [10] (BBM) for description of the Coulomb- induced dissociation of projectile, the eikonal approximation of the Glauber model [11] (EAGM), and the Green function method with one final state interaction in the  $^{15}\text{O}$ -p subsystem [6] (OFSI model).

For quantitative estimates of the Coulomb-nuclear interference, the total excitation cross section to the  $^{15}\text{O}+p$  channel is written as

$$\frac{d\sigma_{dif}(E_T, \theta)}{dE_T d\theta} = |A_C(E_T, \theta) + A_N(E_T, \theta)|^2, \quad (1)$$

where  $A_C(E_T, \theta)$  and  $A_N(E_T, \theta)$  are the Coulomb and nuclear amplitudes depending on the  $^{17}\text{Ne}$  energy  $E_T$  (calculated from the  $^{15}\text{O}+p+p$  threshold) and scattering angle  $\theta$  in the laboratory system, approximated as

$$A_C \approx \sqrt{\frac{d\sigma_{dif}^C}{d\theta} \frac{dB_C}{B_C dE_T} F_{abs}(\theta)} ; \quad A_N \approx e^{i\phi_{rel}} \sqrt{\frac{d\sigma_{dif}^N}{d\theta} \frac{dB_N}{B_N dE_T}} \quad (2)$$

Here,  $\phi_{rel}$  is the relative Coulomb-nuclear phase-shift, a free parameter (generally depending on  $E_T$ ),  $B_C(E\lambda, E_T)$  and  $B_N(E\lambda, E_T)$  are the strength functions of the Coulomb and nuclear-induced excitations with multipolarity  $\lambda$ , depending the  $^{17}\text{Ne}$  energy  $E_T$ .

The *first modification* we use in calculations of the Coulomb excitation cross section  $\sigma_{dif}^C$  in BBM is that the stepwise function at minimal impact parameter (corresponding to the grazing angle) is replaced by a smooth function  $F_{abs}(b)$  describing the absorption of  $^{17}\text{Ne}$  by the target and taking into account the diffusive edge of the nucleus. It is defined in EAGM as  $F_{abs}(b) = \langle |S_{p1} S_{p2} S_C|^2 \rangle$ , profile functions of the proton-target ( $S_{pi}$ ,  $i = 1, 2$ ) and  $^{15}\text{O}$  core-target ( $S_C$ ) interactions [11] are determined by the corresponding interaction potentials and fragment densities with parameters fitted to reproduce the interaction cross section (see Fig. 1). Fig. 1 shows sensitivity of cross sections calculated in EAGM to the profile functions, in particular, to the size of the  $^{15}\text{O}$  fragment. For this, two values of the  $^{15}\text{O}$  rms radius are used in the calculations, 2.42 fm and 2.51 fm [12]. For the parameters we refer to [9, 13, 14].

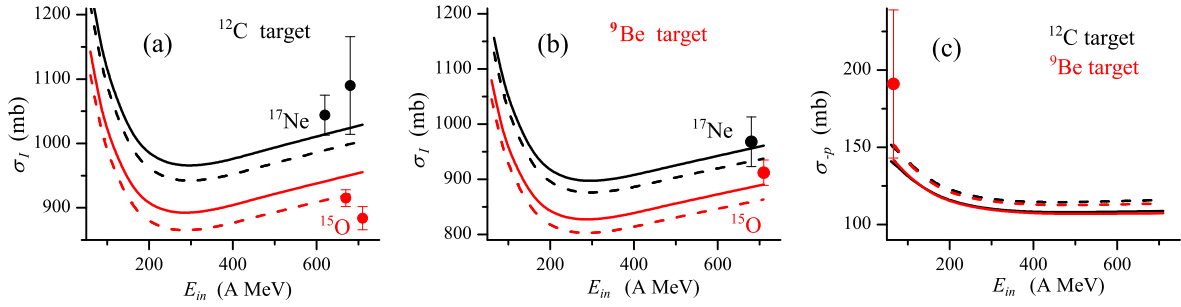


**Figure 1.** Energy dependence of the  $^{15}\text{O}$  (red curves) and  $^{17}\text{Ne}$  (black curves) interaction cross sections on the  $^9\text{Be}$  (a) and  $^{12}\text{C}$  (b) targets obtained with the reduced core rms radius (solid lines) and free nucleus rms radius (dashed lines); energy dependence (c) of the two-proton removal cross section in the Be (black curves) and C (red curves) targets. Experimental data are from [15].

To rewrite  $F_{abs}(b)$  as a function of the angle  $\theta$  we make the *second modification*: angular distributions in nuclear-induced dissociation are defined by the Coulomb trajectories and the impact parameter  $b$  is related to the angle  $\theta$  as  $b(\theta) = a \cot \theta/2$  (in non-relativistic limit) where  $a$  is a constant [10]. In this case, the free parameter of the BBM, the impact parameter corresponding to the grazing angle, is now fixed in our approach by the profile functions. The nuclear differential diffraction cross section  $d\sigma_{dif}^N/d\theta$  for  $^{17}\text{Ne}$  takes the form [11]

$$\frac{d\sigma_{dif}^N}{d\theta} = 2\pi \sin \theta \left\{ \langle |1 - S_{n_1} S_{n_2} S_C|^2 \rangle - \langle |1 - S_{n_1} S_{n_2} S_C \rangle|^2 \right\} \quad (3)$$

where  $\langle \rangle$  denotes the ground-state expectation value. Note that in the calculations we use the  $^{17}\text{Ne}$  ground state WF obtained in [3] with the method of the Hyperspherical Harmonics [16]. This wave function provides 48% weight of s-wave configurations.

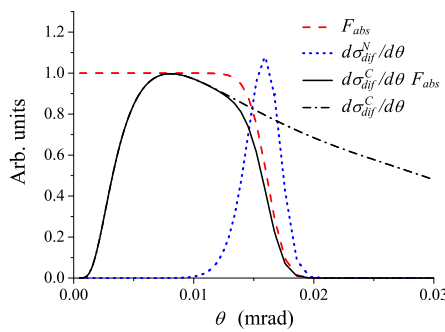


**Figure 2.** Angular dependence of electromagnetic dissociation cross section  $d\sigma_{dif}^C/d\theta$  (dash-dotted black line) and that corrected by nuclear absorption (solid black line),  $F_{abs}(b)$  (dashed red line), and nuclear dissociation cross section  $d\sigma_{dif}^N/d\theta$  (blue dotted line).

The angular dependence of  $F_{abs}$ , the nuclear diffraction cross section obtained in the EAGM and the E1 Coulomb dissociation cross section calculated in BBM are given for lead target in Fig. 2. The nuclear diffraction takes place at the surface of the nucleus leading to larger reflection angles than those corresponding to the Coulomb dissociation. With the diffusive nuclear edge there is a region of angles where both the Coulomb and nuclear mechanisms acts and may interfere. Note, that all calculations were made for the  $^{17}\text{Ne}$  incoming energy  $E_{in}=500$  A MeV.

To estimate the Coulomb-nuclear interference using (2) we need the strength function for nuclear-induced excitation. Calculations of the strength function in the OFSI model [6] are rather complicated, and we use the *third simplification* supposing that  $B_C(E\lambda, E_T)$  and

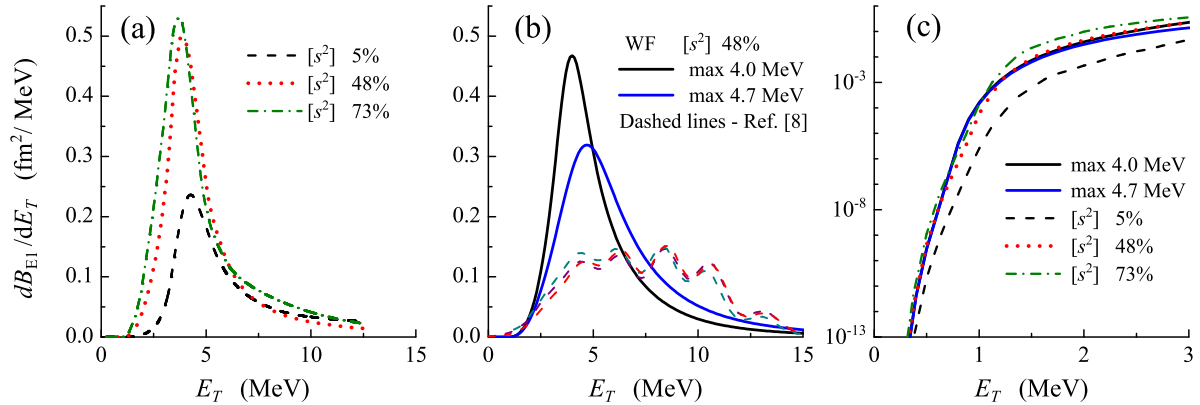


**Figure 3.** (a) - strength functions obtained in [6] with different ground state wave functions of  $^{17}\text{Ne}$  with different weights of s and d-waves; (b) - strength functions obtained within our approach with different FSI (shown by solid lines) in the comparison with results of the RPA model (shown with dashed lines) [7]; (c) - low energy behavior of our strength functions compared with those obtained in [6].

$B_N(E\lambda, E_T)$  are similar. Here, the energy  $E_T$  dependence of the strength function is calculated in the OFSI model with the total strengths of the  $^{17}\text{Ne}$  Coulomb excitation taken from Refs. [17]. The E1 strength function is found as

$$\frac{dB_{E1}}{dE} = 2 \frac{2J_f + 1}{2J_i + 1} \left( \frac{2}{\pi} \right)^2 E_T \int_0^1 d\varepsilon \frac{|A(\varepsilon)|^2}{v_X v_Y} \quad (4)$$

where energy  $E_T = E_X + E_Y$  is the sum of energies in the X- and Y- subsystems ( $^{15}\text{O} + \text{p}$  and  $^{16}\text{F} + \text{p}$ , respectively),  $\varepsilon = E_X/E_T$ ,  $v_X$  and  $v_Y$  are corresponding relative velocities of the fragments in the subsystems (for more details of the OFSI model we refer to [6]). The amplitude of excitation  $A(\varepsilon)$  is determined by the  $^{17}\text{Ne}$  WF and the dipole operator written in the Jacobi coordinates as  $\hat{D}_\mu = Z_{eff} \rho \cos \theta Y_{1\mu}(\hat{\mathbf{y}})$  with  $Z_{eff} = e^2 \frac{98}{255}$ .

Calculations within the OFSI model are performed taking into account the antisymmetrization for excited state WFs, the recoil effects for different components, depending on the spin in the subsystems. Also the resonances in the s- and d-waves of the core-p subsystem are taken into account (one final state interaction). In Fig. 3 the calculated strength functions of  $^{17}\text{Ne}$  are compared with the results of other authors [6, 7]. In panel (a) strength functions from [6] are shown, obtained with three different ground state wave functions of  $^{17}\text{Ne}$  containing respectively  $\sim 5\%$ ,  $\sim 48\%$ , and  $\sim 73\%$  of the  $[s^2]$  configuration in the three-body calculations. In panel (b) of this figure the blue and black solid curves are obtained for the ground state WF ( $[s^2] \sim 48\%$ ) with different p-wave interaction potentials in the Y-subsystem ( $^{16}\text{F}$  subsystem and the proton), showing the sensitivity of the results to this final state interaction. Thus, varying the potential in Y-subsystem we change the position of the maximum of the strength function from 4.0 MeV to 4.7 MeV. These results in (b) are compared with those, obtained within RPA collective-type model [7]. In panel (c) our results (solid lines) are compared to those from [6] (dashed lines) at low energies.

Finally, writing the expression for differential cross section  $d\sigma_{dif}^N(J, J', P)/d\theta$  of the transition from the ground state  $J$  to the excited state  $J'$  for the certain multipolarity  $\mathbf{P}$  of the nuclear-induced excitation  $N_P$ , it is possible to deduce transition rules for change in parity  $\pi\pi' = (-1)^P$  and  $\mathbf{J}' = \mathbf{P} + \mathbf{J}$ , and find the N1 contribution to the cross section of nuclear-induced excitation to the state  $J'$  depending on the angle  $\theta$  and energy  $E_T$ .

**Table 1.** Total cross section, cross sections of the Soft E1 and N1 excitation, cross sections of the Soft E1 and N1 excitation leading to the  $^{16}\text{F}$  production in s-wave and d-wave resonant states in C, Si, and Pb targets at the  $^{17}\text{Ne}$  energy 500 A MeV. All the cross sections are given in mb.

target	$\sigma_{diff}^C$ total	$\sigma_{diff}^C$ E1	$\sigma_{diff}^C$ E1, s	$\sigma_{diff}^C$ E1, d	$\sigma_{diff}^N$ total	$\sigma_{diff}^N$ N1	$\sigma_{diff}^N$ N1, s	$\sigma_{diff}^N$ N1, d
Pb	415	386	368	18	35	1.2	0.1	0.05
Si	17	15	14.3	0.71	13	0.5	0.04	0.02
C	3.2	3.0	2.86	0.14	12	0.4	0.03	0.016

### 3. Results

The results of the total Coulomb and nuclear cross section calculations are presented in Table 1. For the lead target, the contribution of the N1 nuclear transition is negligibly small compared to that of E1. Depending on the phase  $\phi_{rel}$  in (2) the corresponding deviation from the decoherent value with  $\phi_{rel} = \pi/2$  is within 3% for the Pb target, 12% for the Si target, and 15% for the C target. Note, that in the  $^{17}\text{Ne}$  Coulomb dissociation, the spectra of the  $^{16}\text{F}$  production in the s- and d-wave resonant states have their maxima at  $\sim 4.5$  MeV and  $\sim 6.5$  MeV, respectively. The d-wave  $^{16}\text{F}$  production is small in the whole range of the  $^{17}\text{Ne}$  energy  $E_T$  for both C and Pb targets, and the shape of the SDM peak is mainly determined by the s-wave  $^{16}\text{F}$  production.

Using our strength functions  $\frac{dB_{E1}}{dE}$  (Fig. 3 (b)) we estimate the non-resonant E1 contribution to the  $^{15}\text{O}(2p, \gamma)^{17}\text{Ne}$  reaction rate as function of the temperature  $T$  [6]

$$\langle \sigma_{2p, \gamma v} \rangle = \left( \frac{17}{15} \right)^{3/2} \left( \frac{2\pi}{mkT} \right)^3 \frac{2J_f + 1}{2(2J_i + 1)} \int dE \frac{16\pi}{9} e^2 E_\gamma^3 \frac{dB_{E1}(E)}{dE} \exp \left[ -\frac{E}{kT} \right] \quad (5)$$

where  $J_i$  and  $J_f$  are spins of  $^{15}\text{O}$  and  $^{17}\text{Ne}$  g.s.,  $k = 8,6173324(78)10^{-5}$  eV/K is the Boltzmann constant.

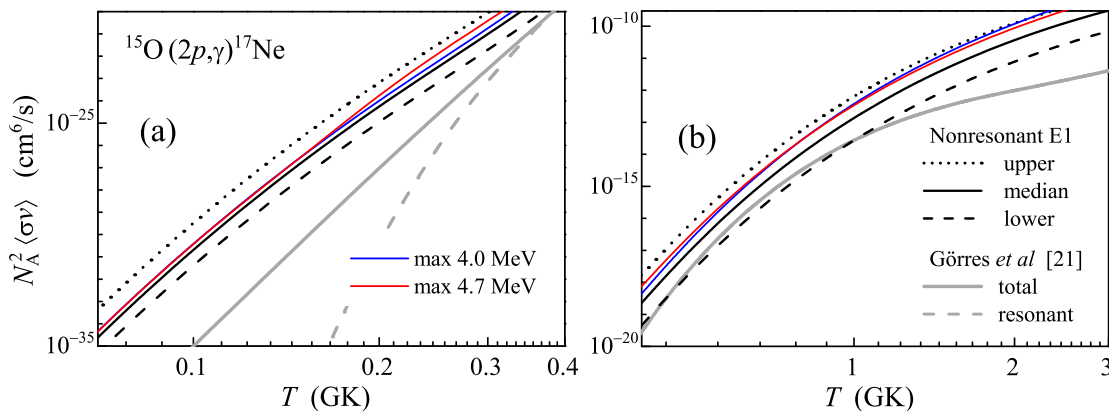


**Figure 4.** Temperature dependence of the astrophysical rate. Rate 1(2) is shown by blue(red) line. Black curves from [6] are the median (solid line) rate and its upper (dashed line) and lower (dotted line) limits obtained with regard for uncertainties in calculated resonance and non-resonant contributions. Grey curves are total intensity and resonance contribution from Ref. [18].

Figure 4 shows the 2p-capture rate in different temperature regions obtained with the strength functions with maxima at 4.0 and 4.7 MeV. One can see, that the results of our calculations with the WF providing 48% of s-wave are very close to the curves from [6] obtained with the same WF within the same, OFSI, model, but without considering for antisymmetrization of the excited state wave function and recoil effects. From comparison of the red and blue lines, we see, that the final state p-wave interaction potentials in the Y-subsystem, determining the position of the SDM peak, insufficiently affects our results at the energies  $E_T$  up to resonance (the difference does not exceed 2 times). At the same time, our results and those from [6] exceeds the results from [18] by few orders of magnitude.

#### 4. Conclusions

The Coulomb-nuclear interference is estimated for the first time for three-body  $^{17}\text{Ne}$  dissociation. The applied approach provides a quite realistic description of the E1 Coulomb and N1 nuclear excitation of the  $^{17}\text{Ne}$  Borromean nucleus. In the calculations of the 2p-capture rates at astrophysical (low) energies the OFSI model shows to be a reliable substitute for the full three-body model [6], with transparent physical interpretation. In our approach we got, that in the calculations with the same three-body WF, the 2p-capture rate at low temperature ( $< 0.2$  GK) is independent of the position of the maximum of the strength function related with the p-wave potential in the Y-subsystem ( $^{16}\text{F}$  subsystem and the proton). At higher temperatures, there is a relation between the p-wave potential in the Y-subsystem ( $^{16}\text{F}$  subsystem and the proton) and the position of the maximum of the SDM strength function. The shape of the calculated  $^{17}\text{Ne}$  excitation spectrum is related to the shape of the strength function obtained within the OFSI model, having maximum at about 4 - 5 MeV. Thus, knowing the experimental spectrum of the "Soft E1" mode and its maximum position it will be possible to restore the E1 strength function and to make more precise assessment of the 2p-capture rates.

Besides this, it appeared that in the  $^{17}\text{Ne}$  excitation, the Coulomb-nuclear interference in a heavy target like lead target is small due to negligible nuclear contribution compared to the Coulomb one.

It is also important to point out the restrictions of our approach related to simplifications noted above, i.e. the strength function of the nuclear N1 excitation can differ from the E1 Coulomb one, the final state interaction should be taken into account for all fragments.

#### References

- [1] Grigorenko L V 2009, *Physics of Particles and Nuclei* **40** 674
- [2] Goldansky V I 1960, *Nucl. Phys.* **19** 482
- [3] Grigorenko L V *et al.* 2003 *Nucl. Phys.* **A713** 372; erratum 2004 *Nucl. Phys.* **A740** 401
- [4] Aumann T, *et al.* 2012 *Journal of Physics: Conference Series* **337** 012011
- [5] Ikeda I 1988 INS, JPH-7, 1988 (in Japanese) ; Hansen P and Jonson B 1987 *Europhys. Lett.* **4** 409
- [6] Grigorenko L V *et al.* 2006 *Phys. Lett.* **B641** 254
- [7] Oishi T, Hagino K and Sagawa H 2011 *Phys. Rev. C* **84** 057301
- [8] Grigorenko L V, Parfenova Yu L and Zhukov M V 2005 *Phys. Rev. C* **71** 051604(R)
- [9] Parfenova Y L and Zhukov M V 2005 *AIP Conf. Proc. FINUSTAR (Greece)* **831** 526
- [10] Bertulani C A and Baur G 1988 *Phys. Rep.* **163** 299
- [11] Bertch G F, Hencken K and Esbensen H 1998 *Phys. Rev. C* **57** 1366
- [12] Parfenova Yu L, Zhukov M V and Vaagen J S 2000 *Phys. Rev. C* **62** 044602
- [13] Parfenova Y L and Zhukov M V 2006 *Phys. Rev. C* **74** 054607
- [14] Grigorenko L V, Parfenova Y L and Zhukov M V 2005 *Phys. Rev. C* **71** 051604R
- [15] Ozawa A, Suzuki T and Tanihata I 2001 *Nucl. Phys.* **A693** 32
- [16] Zhukov M V *et al.* 1993 *Phys. Rep.* **231** 151 ; Danilin B V *et al.* 1989 *Yad. Fiz.* **49** 351 (*Sov. J. Nucl. Phys.* **49** 351)
- [17] Chromik M J *et al.* 1997 *Phys. Rev. C* **55** 1676 ; Chromik M J *et al.* 2002 *Phys. Rev. C* **66** 024313
- [18] Görres *et al.* 1995 *Phys. Rev. C* **51** 392